# IGR J19294+1816: a new Be-X-ray binary revealed through infrared spectroscopy

J. J. Rodes-Roca,[1,2]⋆ G. Bernabeu,[1,2]⋆ A. Magazzù,[3] J. M. Torrejón[1,2]⋆ and E. Solano[4,5]

[1]*Department of Physics, Systems Engineering and Signal Theory, University of Alicante, E-03080 Alicante, Spain*
[2]*University Institute of Physics Applied to Sciences and Technologies, University of Alicante, E-03080 Alicante, Spain*
[3]*Telescopio Nazionale Galileo, Rambla José Ana Fernández Pérez, E-38712 Breña Baja, Spain*
[4]*Departamento de Astrofísica, CAB (CSIC-INTA), ESA-ESAC Camino Bajo del Castillo s/n, E-28692 Villanueva de la Cañada, Madrid, Spain*
[5]*Spanish Virtual Observatory, E-28691 Villanueva de la Cañada, Madrid, Spain*

## ABSTRACT

The aim of this work is to characterize the counterpart to the *INTErnational Gamma-Ray Astrophysics Laboratory* high-mass X-ray binary candidate IGR J19294+1816 so as to establish its true nature. We obtained *H*-band spectra of the selected counterpart acquired with the Near Infrared Camera and Spectrograph instrument mounted on the Telescopio Nazionale Galileo 3.5-m telescope which represents the first infrared spectrum ever taken of this source. We complement the spectral analysis with infrared photometry from UKIDSS, 2MASS, *WISE*, and *NEOWISE* data bases. We classify the mass donor as a Be star. Subsequently, we compute its distance by properly taking into account the contamination produced by the circumstellar envelope. The findings indicate that IGR J19294+1816 is a transient source with a B1Ve donor at a distance of $d = 11 \pm 1$ kpc, and luminosities of the order of $10^{36-37}$ erg s$^{-1}$, displaying the typical behaviour of a Be-X-ray binary.

**Key words:** stars: emission-line, Be – infrared: stars – X-rays: binaries.

## 1 INTRODUCTION

Current X-ray observatories such as the European Space Agency's (ESA) *INTErnational Gamma-Ray Astrophysics Laboratory* (INTEGRAL; Winkler et al. 2003) or *XMM–Newton* (Watson et al. 2009) have discovered new kinds of high-energy emitters. To characterize the nature of these systems it is mandatory to carry out a multiwavelength study and establish a clear identification of the optical/infrared counterpart.

High-mass X-ray binaries (HMXBs) are X-ray sources fed by accretion of material from a donor OB star on to a compact object (a black hole or a neutron star). They are primary astrophysical laboratories where fundamental properties can be tested, such as the following: the masses of neutron stars and the equation state of the nuclear matter; the structure of the stellar wind in massive stars; or, the evolutionary paths of binary systems. (Martínez-Núñez et al. 2017). Until recently, three main kinds of HMXBs were known:

(i) The largest group has a Be star as a donor. These systems are called BeX systems (Reig 2011). A Be star is a main-sequence or giant star which harbours a circumstellar equatorial disc. These systems are transient (in X-rays) with a duration of some weeks

and show luminosities of $L_X \sim 10^{36}$–$10^{37}$ erg s$^{-1}$. Approximately 70 per cent of all known X-ray pulsars belong to this class.

(ii) An increasing number of sources have a supergiant OB donor (SGXBs or SFXTs). SGXBs are persistent sources where the compact object accretes material from the powerful stellar wind, producing luminosities of the order of $L_X \sim 10^{36}$ erg s$^{-1}$. SFXTs are transient sources showing luminosities of $L_X \sim 10^{33-34}$ erg s$^{-1}$ during quiescence that can increase by up to four orders of magnitude in very short time-scales.

(iii) A very small group where the transfer of mass is directly from the surface of the donor star (Roche lobe overflow). This evolutionary phase is very short and is consequently very scarce. For instance, in the Milky Way only the Cen X-3 is presently observable.

The population synthesis models that were previously available seemed to reproduce the distribution well. For example, the brevity of the supergiant phase was reflected in the small number of SGXBs detected. However, with the discovery of an increasing number of obscured sources by high-energy satellites like ESA's *INTEGRAL* gamma-ray telescope, the population synthesis models started to change. Given the *INTEGRAL*'s sensitivity above 20 keV and its observing strategy, which produce very long exposure times specifically towards the Galactic Centre, new sources were discovered, that had been missed in the past due to the very high absorption or the very short transient nature. The majority of these newly discovered

⋆ E-mail: rodes@dfists.ua.es (JJR-R); bernabeu@ua.es (GB); jmt@ua.es (JMT)

sources had supergiant donors. The persistent sources dramatically increased the number of SGXBs. As an example, we identified the *XMM–Newton* source 2XMM J191043.4+091629 with a distant SGXB (Rodes-Roca et al. 2013) which helps to independently trace the galactic structure. It also contains the slowest pulsar found to date (Sidoli et al. 2017). Furthermore, the transient systems revealed an entirely new class of objects, the Supergiant Fast X-ray Transients (SFXTs). Finally, we have discovered obscured BeX systems (main-sequence donors) close to earth. All these discoveries can challenge the population synthesis models. Therefore, to characterize as many counterparts as possible is very important.

Often these new sources turn out to be highly absorbed. The spectral classification using the blue band would require very long exposure times on large telescopes or it is not feasible. However, they can be perfectly observed with the IR instrumentation on a 4-m class telescope. The spectral classification of hot stars can be achieved with *H*-band spectra (Hanson, Rieke & Luhman 1998). Together with available infrared photometry and the X-ray behaviour, the nature of the system can be established unambiguously.

IGR J19294+1816 was discovered by the *IBIS/ISGRI* imager on-board *INTEGRAL* during an observation of the field around GRS 1915+105 on March 27, 2009 (Turler, Rodriguez & Ferrigno 2009). Using *Swift/XRT* archival observations, Rodriguez et al. (2009b) gave a refined X-ray position identified with the source named Swift J1929.8+1818 ($\alpha = 19^\mathrm{h}29^\mathrm{m}56^\mathrm{s}$ and $\delta = +18°18'38''$ with an uncertainty of 3.5 arcsec at 90 per cent confidence level). The single star falling in the *XRT* error circle was identified as the IR counterpart to the X-ray source, and associated with 2MASS J19295591+1818382. However, no optical or radio counterpart was found in any other catalogues they searched for. The *XRT* spectrum is well described by an absorbed power law or by a single absorbed blackbody. The timing analysis revealed the presence of a pulse around 12.43 s which was later confirmed with *RXTE* (Strohmayer et al. 2009). The X-ray source displays short outbursts (several thousand seconds) which suggested initially a SFXT nature (Rodriguez et al. 2009a). Bozzo et al. (2011), from *INTEGRAL* and *Swift* observations, concluded that the X-ray source showed a behaviour reminiscent of a Be-X-ray binary system.

In this work, we present the first ever infrared spectrum of IGR J19294+1816[1] supported by the analysis of archival IR photometry in order to ascertain the true nature of the source. In Section 2, we describe the IR observations. In Section 3, we present our results and, finally, we present our conclusions in Section 4.

## 2 OBSERVATIONS AND DATA REDUCTION

### 2.1 TNG observations

Near-IR spectroscopy was obtained during the night of 2014 September 1, using the Near Infrared Camera and Spectrograph (NICS) mounted at the 3.5-m Telescopio Nazionale Galileo (TNG) telescope (La Palma island). Medium-resolution spectra were taken with the *H* grism under good seeing conditions and reasonable signal-to-noise (S/N) ratio of 100.

To remove the sky background, the target and the standard stars were observed according to a nodding ABBA sequence along the slit, using an automatic script available at the telescope. Consequently, each observation consisted of four images with the source

spectrum displaced at different positions on the detector. The separation between the A and B positions was 15 arcsec.

As the first step of the reduction process, possible cross-talking effects were removed using a Fortran program available from the TNG web pages. Secondly, background subtraction was made by taking (A−B) and (B−A) image differences, obtaining four positive aperture images. The AB and BA sequences were so close in time that sky background variation between them was negligible. This method, together with the use of the 1.0 arcsec slit, also minimizes any possible nebular contamination.

For each differential image, a spectrum was extracted using the *apall* task in the IRAF[2] environment. During the extraction, we removed the residual background and traced the apertures along the dispersion. The four extracted spectra of each group were then combined together with a median algorithm to produce a single spectrum, thereby eliminating cosmic ray spikes.

To remove the telluric features, a number of A0V stars were observed throughout the night at similar airmasses as the targets. These spectra were fitted with a theoretical spectrum corrected for rotation and radial velocity. The standard spectra were divided by the model isolating the telluric spectrum which was used subsequently to correct the target spectra. We carefully checked that division by the telluric spectrum does not introduce any spurious features. At our resolution (3.5 Å pix$^{-1}$), this method works very well for the *H* band. However, it could somewhat increase the emission lines seen in the *K* band, although we estimate this effect to be smaller than 20 per cent in Br$\gamma$. In this paper, we are concerned with the characterization of the donor. As will be shown, it turns out to be a Be star. In the IR essentially, we are seeing the circumstellar envelope emission and, consequently, the line ratios cannot be used for spectral classification. Therefore, we have not corrected further for this effect.[3] The final spectra are shown in Fig. 1.

## 3 DATA ANALYSIS

### 3.1 Near-IR spectra and classification of the counterpart

The spectral analysis was carried out using the STARLINK[4] software and the IRAF package.[5] To identify the emission/absorption lines and spectral classification, we used the following atlases: Blum et al. (1997), Meyer et al. (1998), and Hanson et al. (1998) for the *H* band; Hanson, Conti & Rieke (1996) and Hanson et al. (2005) for the *K* band.

Fig. 1 shows our *H*-band *TNG* spectrum. To date, this is the only infrared spectrum obtained for this source. The strong absorption (see Section 3.2) $A_V^\mathrm{tot} = 15.7 = 3.1\,E(B-V)$ implies a colour excess of $E(B-V) = 5.1$ and makes it difficult to obtain an optical blue spectrum with a 4-m class telescope. The NIR *H*-band spectrum exhibits the presence of the Brackett H I series from Br(19–4) line at 1.5235 μm to the Br(10–4) transition at 1.7362 μm. This points clearly towards an early B type star, since these lines disappear for O type stars. All these lines are in emission. The

---

[2] Image Reduction and Analysis Facility is written and supported by the National Optical Astronomy Observatories which is operated by the Association of Universities for Research in Astronomy, Inc. under cooperative agreement with the National Science Foundation.

[3] The corrected spectra will be used to diagnose specifically the physical properties of the circumstellar envelopes. However, this is beyond the scope of this paper.

[4] http://starlink.jach.hawaii.edu/starlink

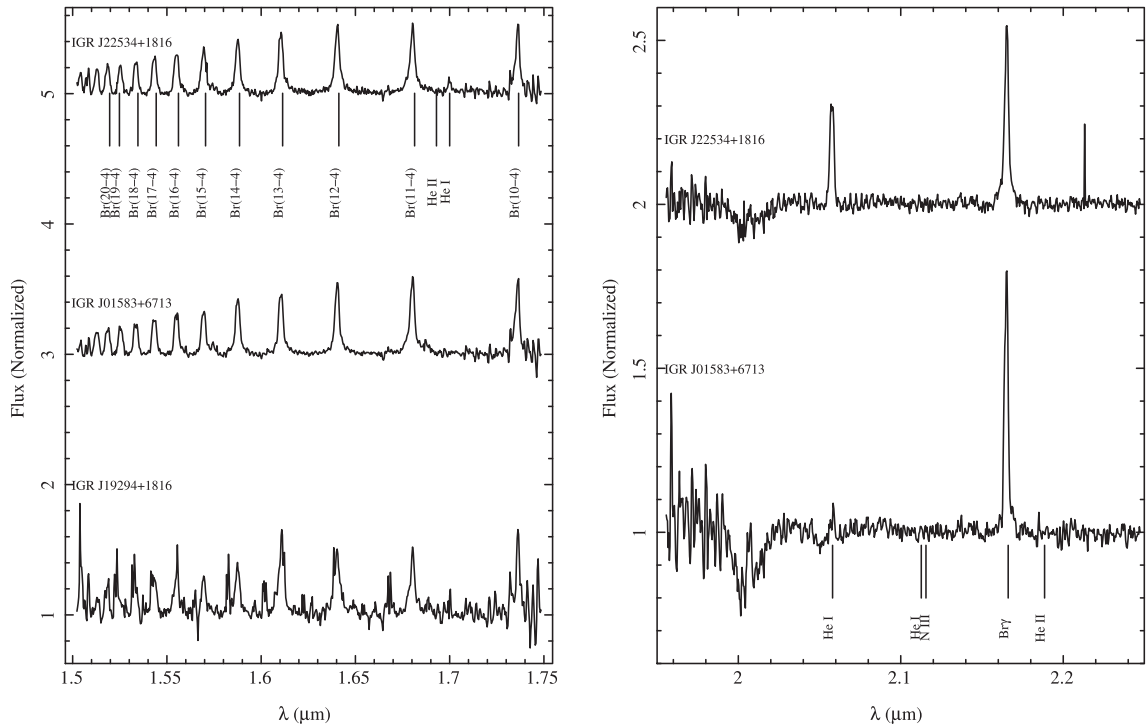[5] http://iraf.noao.edu

[1] http://irfu.cea.fr/Sap/IGR-Sources

**Figure 1.** NIR spectra of the counterparts to the X-ray binaries. No other emission or absorption lines were detected apart from Brackett series of H I and He I 2.058 μm emission lines. Note the absence of any feature at the position of the He II 2.1885 μm line.

1.700 μm He I line is seen also in emission. This is typical of Be stars in which the circumstellar disc emission dominates the spectrum at NIR wavelengths. Some Brackett series lines show a double peak structure. According to a few analyses of infrared emission line profiles in Be stars, they have the same characteristics as those in the visible region (Underhill & Doazan 1982). Most Be stars show double-peak structure in their Balmer emission lines (Slettebak, Collins & Truax 1992). In general, this double-peak structure is to be expected for a rotating emitting disc. If the star is viewed at an intermediate angle of inclination of the line of sight on the rotation axis, the emission lines exhibit a weak central reversal typical of a Be spectrum. Features at 1.5965 μm [Fe II], at 1.6027 μm C I (possibly blended with 1.6002 μm [Fe II] and/or 1.6009 μm C I) and at 1.6685 μm Si I seem to be present in our spectrum. Another line could match the position of He II at 1.697 μm. He II is only detected in O stars, and preferentially in the supergiants (Hanson et al. 1998). However, He II is very weak preventing differentiation from the continuum noise level. Furthermore, *H*-band spectra of Be stars show all Brackett series in emission Steele & Clark (2001). At any rate, the *H*-band spectrum seems to be characteristic of a Be star.

As a comparison, we also show for the first time NIR spectra of two previously classified Be-X-ray binaries based on optical spectra. For IGR J01583+6713, Halpern & Tyagi (2005) obtained a low-resolution optical spectrum which revealed strong H $\alpha$ and weak H $\beta$ emission lines, of equivalent width (EW) 70 and 6 Å, respectively, as well as diffuse interstellar bands. These features suggested a Be companion. Subsequent optical spectroscopy (Masetti et al. 2006; Kaur et al. 2008) confirmed its Be-X nature. For IGR J22534+6243, Masetti et al. (2012) obtained a spectrum of a highly reddened, intrinsically blue continuum star with superimposed H $\alpha$, H $\beta$, and He I emission lines pointing strongly to a Be companion. Esposito et al. (2013) confirmed the Be-X nature using

**Table 1.** *H*- and *K*-band line identifications for each source which the corresponding equivalent widths.

| Emission line | Wavelength (μm) | IGR J 01583+6713 | 19294+1816 EW (Å) | 22534+6243 |
|---|---|---|---|---|
| Br 20 | 1.5196 | $-5.5 \pm 0.8$ | $-5.5 \pm 0.8$ | $-5.9 \pm 0.8$ |
| Br 19 | 1.5265 | $-5.7 \pm 0.8$ | $-9.3 \pm 1.3$ | $-5.5 \pm 0.8$ |
| Br 18 | 1.5346 | $-7.0 \pm 1.0$ | $-9.5 \pm 1.4$ | $-7.0 \pm 1.0$ |
| Br 17 | 1.5443 | $-8.2 \pm 1.2$ | $-10.6 \pm 1.5$ | $-8.5 \pm 1.2$ |
| Br 16 | 1.5561 | $-9.9 \pm 1.4$ | $-10.8 \pm 1.5$ | $-10.3 \pm 1.5$ |
| Br 15 | 1.5705 | $-10.5 \pm 1.5$ | $-7.5 \pm 1.1$ | $-11.4 \pm 1.6$ |
| Br 14 | 1.5885 | $-14.8 \pm 2.1$ | $-11.6 \pm 1.7$ | $-14.7 \pm 2.1$ |
| Fe II | 1.5965 | – | $-1.4 \pm 0.2$ | – |
| Fe II | 1.6019 | – | Blended? | – |
| C I | 1.6027 | – | $-5.1 \pm 0.7$ | – |
| Br 13 | 1.6114 | $-14.9 \pm 2.1$ | $-20 \pm 3$ | $-16.7 \pm 2.4$ |
| Br 12 | 1.6412 | $-19 \pm 3$ | $-21 \pm 3$ | $-19 \pm 3$ |
| Si I | 1.6685 | – | $-4.7 \pm 0.7$ | – |
| Br 11 | 1.6811 | $-22 \pm 3$ | $-17.4 \pm 2.4$ | $-21 \pm 3$ |
| He I | 1.7007 | – | $-1.4 \pm 0.2$ | $-2.3 \pm 0.3$ |
| Br 10 | 1.7362 | $-19 \pm 3$ | $-14.9 \pm 2.1$ | $-16.2 \pm 2.3$ |
| He I | 2.0580 | $-1.3 \pm 0.2$ | – | $-9.9 \pm 1.4$ |
| He I | 2.1126 | $<-0.2$ | – | $<-0.3$ |
| N III | 2.1155 | $<-0.2$ | – | $<-0.1$ |
| Br $\gamma$ | 2.1661 | $-24 \pm 3$ | – | $-20 \pm 3$ |
| He II | 2.1885 | $<-0.2$ | – | $<-0.4$ |

a blue band spectrum of the IR counterpart obtained with the 2.5-m Nordic Optical Telescope (NOT, La Palma). Although the S/N is poorer for IGR J19294+1816 (because it is 2 magnitudes fainter in *H*) it is clearly consistent with a Be donor.

Table 1 summarizes the line identifications and the estimated equivalent widths for all the observed targets.
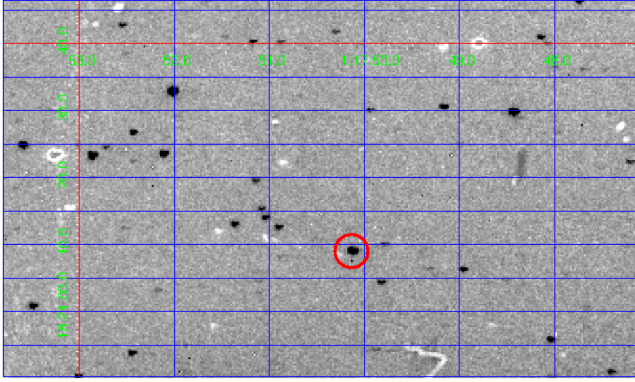
**Figure 2.** TNG *K*-band image of the region with the counterpart marked (red circle). The white dots are ghosts due to imperfect subtraction of the images during dithering. However, the image was used only for object identification and not for photometric analysis. North is up, East is left.

In order to rule out any contamination by an unresolved companion, we compared the same field of view in the *K* band of 2MASS and UKIDSS as this last survey provides a higher angular resolution. This is a necessary test for faint sources (typically $K > 10$ mag) as we demonstrated in Rodes-Roca et al. (2013). The source is not blended, as it shown in Fig. 2.

In summary, the NIR spectrum of IGR J19294+1816 points strongly towards a Be nature of the donor. This conclusion is further strengthened by the photometry presented in the next section.

### 3.2 Photometry

To carry out the photometric analysis we used the Simbad data base (Wenger et al. 2000), several optical data bases, such as *Gaia* (Gaia Collaboration 2016a,b; Evans et al. 2017; van Leeuwen et al. 2017), *IPHAS* (Drew et al. 2005), and *PAN-STARRS* (Chambers et al. 2016; Flewelling et al. 2016; Magnier et al. 2016a,b,c; Waters et al. 2016), and several IR data bases such as the UK Infrared Telescope (UKIRT) Infrared Deep Sky Survey (UKIDSS; Lawrence et al. 2007), the Two Micron All Sky Survey (2MASS; Skrutskie et al.), the GLIMPSE data base, the *Wide-field Infrared Survey Explorer* (*WISE*) all sky survey (Wright et al. 2010), and the *Near-Earth Object WISE* (*NEOWISE*; Mainzer et al. 2011, 2014) obtaining the photometry given in Table 2.

Classical Be stars tend to occupy a reduced region in the colour–colour (CC) diagram [$W1 - W2$] versus [$W2 - W3$], see figs 5 and 7 central panel in Koenig & Leisawitz (2014). They are located in the range [$-0.1$–0.6] versus [$-0.1$–1.5] in this diagram. We obtained the single exposure data from the *WISE* All-Sky Single Exposure (L1b) data base. Then, we selected cc_flag equal to 0 or h and non-null data for *W3* and did the previous CC diagram on the *IRSA* (Infrared Science Archive) web application (Fig. 3). For the Be-X-ray binaries IGR J01583+6713 and IGR J22534+6243 all the values are found in the classical Be zone.[6] No significant variability was found within the uncertainties. For IGR J19294+1816 the values of the *W3* filter had a spurious detection and only an upper limit on magnitude could be estimated. Therefore, error bars in $W2 - W3$ are the uncertainties measured in *W2*. Nevertheless, the points in the CC diagram were also consistent with a classical Be star.

In addition, the *NEOWISE* data base has single exposure data for these objects allowing us to plot the colour–magnitude (CM)

---

[6] Although can be confused with blue transition disc objects.

**Table 2.** Photometry of candidate counterparts.

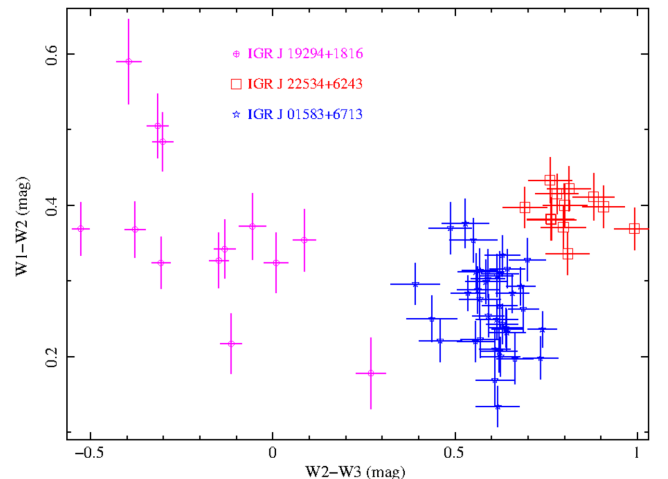| Photometry | IGR J | | |
| --- | --- | --- | --- |
| (mag) | 01583+6713 | 19294+1816 | 22534+6243 |
| *B* | $15.65 \pm 0.08$ | – | $17.38 \pm 0.11$ |
| *V* | $14.43 \pm 0.03$ | – | $15.61 \pm 0.01$ |
| *B − V* | $1.22 \pm 0.11$ | – | $1.77 \pm 0.12$ |
| | | 2MASS | |
| *J* | $11.48 \pm 0.03$ | $14.56 \pm 0.03$ | $11.644 \pm 0.024$ |
| *H* | $11.03 \pm 0.03$ | $12.99 \pm 0.03$ | $10.961 \pm 0.023$ |
| *K* | $10.601 \pm 0.021$ | $12.115 \pm 0.023$ | $10.46 \pm 0.03$ |
| | | UKIDSS | |
| *J* | – | $14.3019 \pm 0.0020$ | – |
| *H* | – | $12.8710 \pm 0.0009$ | – |
| *K* | – | $11.8792 \pm 0.0011$ | – |
| | | *WISE/NEOWISE* | |
| W1 | $10.099 \pm 0.023$ | $10.715 \pm 0.024$ | $9.87 \pm 0.04$ |
| W2 | $9.715 \pm 0.020$ | $10.283 \pm 0.022$ | $9.45 \pm 0.03$ |
| W3 | $8.85 \pm 0.03$ | $10.27 \pm 0.15$ | $8.57 \pm 0.05$ |
| W4 | $8.4 \pm 0.3$ | $<8.74$ | $7.73 \pm 0.19$ |
| | | GLIMPSE | |
| 3.6 μm | – | $10.95 \pm 0.05$ | – |
| 4.5 μm | – | $10.66 \pm 0.05$ | – |
| 5.8 μm | – | $10.39 \pm 0.07$ | – |
| 8.0 μm | – | $10.20 \pm 0.04$ | – |
| | | PAN-STARRS | |
| *g* (0.477 μm) | – | 27.06 | – |
| *r* (0.613 μm) | – | $22.29 \pm 0.16$ | – |
| *i* (0.748 μm) | – | $20.15 \pm 0.05$ | – |
| *z* (0.865 μm) | – | $18.335 \pm 0.014$ | – |
| *y* (0.960 μm) | – | $17.223 \pm 0.014$ | – |
| | | Gaia | |
| *G* (0.673 μm) | – | 20.71 | – |
| | | IPHAS | |
| *i* (0.766 μm) | – | $19.51 \pm 0.08$ | – |



**Figure 3.** *WISE* All-Sky Single Exposure photometry colour–colour diagram.

diagram [$-W1$] versus [$W1-W2$] (Fig. 4). IGR J19294+1816 seems to be quite variable. However, we built the same CM diagram for two nearby sources and also showed the same behaviour (Fig. 5). The standard deviation of the variability in the *WISE* colour is $\overline{W_1 - W_2}_{(IGR)} = 0.1 \pm 0.3$, $\overline{W_1 - W_2}_{(Source1)} = -0.12 \pm 0.14$, $\overline{W_1 - W_2}_{(Source2)} = -0.5 \pm 0.3$, respectively.

As seen in Section 3 all IR lines are in emission. The circumstellar envelope emission contaminates the underlying photospheric
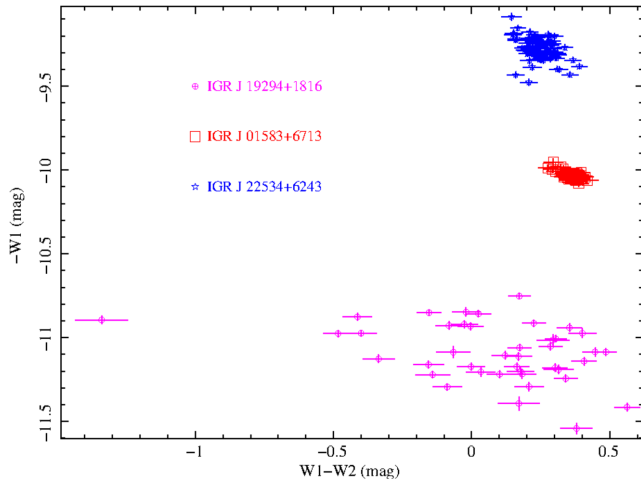
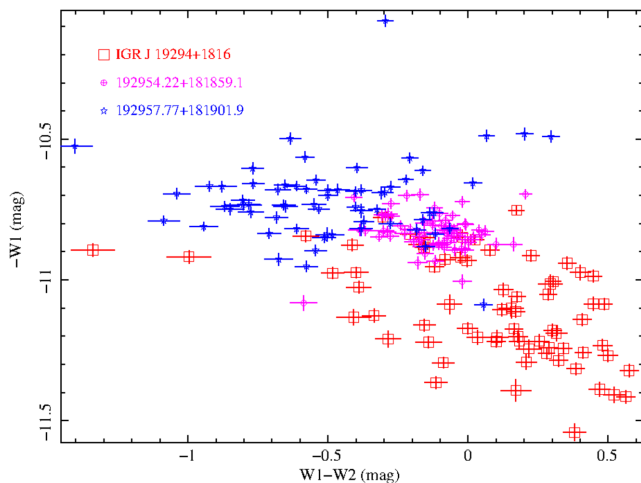**Figure 4.** *NEOWISE* multiepoch photometry colour–magnitude diagram.



**Figure 5.** *NEOWISE* multiepoch photometry colour–magnitude diagram of IGR J19294+1816 and two nearby sources.

spectrum of the Be star and produces an overluminosity (for non-Be-shell) with respect to B stars of the same spectral type and luminosity class. This leads to a systematic under estimation of the distance and, hence, the X-ray luminosity. We will use the recipes given in Riquelme, Torrejón & Negueruela (2012) to correct for these effects. The distance is computed from the usual equation

$$V - M_V - A_V^{\text{tot}} = 5 \log d - 5, \tag{1}$$

where $V$ is the observed magnitude, $M_V$ is the absolute magnitude for the corresponding spectral type and luminosity class and $A_V^{\text{tot}}$ has two terms: the interstellar absorption towards the source $A^{\text{is}} = 3.1 E^{\text{is}}(B - V)$ and the circumstellar *emission*:

$$A_V^{\text{tot}} = \begin{cases} 3.1\, E^{\text{is}}(B-V) - 0.6 \left( \frac{W^{\text{env}}(\text{H}_\alpha)}{-30\,\text{Å}} \right) & \text{if } -W^{\text{env}}(\text{H}_\alpha) < 15\,\text{Å} \\ 3.1\, E^{\text{is}}(B-V) - 0.3 & \text{if } -W^{\text{env}}(\text{H}_\alpha) \geq 15\,\text{Å} \end{cases}. \tag{2}$$

The fact that all the significant lines are in emission implies a well-developed envelope which is responsible for the strong IR excess. Both, IGR J01583+6713 (Halpern & Tyagi 2005) and IGR J22534+6243 (Esposito et al. 2013) have values of measured $-W(\text{H}_\alpha)$ larger than 15 Å (Table 1) and therefore they are in the saturated regime. On the other hand, IGR J19294+1816 presents

also all the significant *H*-band lines in emission, with comparable equivalent widths, demonstrating that the envelope is well developed. We will then assume that this source is also in the saturated regime. In these conditions:

$$A_V^{\text{tot}} = 3.1\, E^{\text{is}}(B - V) - 0.3. \tag{3}$$

IGR J19294+1816 has no *UBV* optical photometry due to the very high extinction. We have derived the excess using the available IR photometry. Be donors in Be-X-ray binaries occupy a rather narrow spectral class interval (Riquelme et al. 2012). We have estimated the distance assuming a B0V or B2V spectral type. In Riquelme et al. (2012) it is shown that the visual to infrared colour circumstellar excess $E(V - I)$ is already three to four times that of $(B - V)$ for Be-X-ray binaries and increases towards longer wavelengths. We estimate that the effect on $(J - K)$ is of the order of 1 magnitude (Riquelme et al. 2012). That is to say $E^{\text{cs}}(J - K) \approx 1$ mag. Therefore $E^{\text{is}}(J - K) \approx E^{\text{tot}}(J - K) - 1$. Following Fitzpatrick (1999) we can compute subsequently $E^{\text{is}}(J - K) = 0.5 E^{\text{is}}(B - V)$ and $A_K^{\text{is}} = 0.36 E^{\text{is}}(B - V)$. In Table 3, we summarize our results. As can be seen, the distances to IGR J19294+1816 are in the range 10–12 kpc. We will assign finally a distance $d = 11 \pm 1$ kpc locating the system at the far edge of the Perseus arm. The line of sight passes through the Sagittarius arm tangentially and the Perseus arm, explaining the high extinction. Using the values from table 4 in Riquelme et al. (2012) and equation (1), we estimate a lower limit for the visual magnitude of $V \sim 23.4$ mag. This is corroborated by the SED analysis in the next section.

### 3.3 Spectral energy distribution

In order to extend the characterization of IGR J19294+1816, we will use the spectral energy distribution (SED) using the photometry on Table 2. It is well known, however, that free–free transitions in the circumstellar envelope of the Be stars produce an excess of photons at long wavelengths with respect to what can be expected from the photospheric flux. The photometric points affected by this *infrared excess* cannot be taken into account in the SED fitting process.

The SED of the source is reported in Fig. 6. We built it using the Virtual Observatory (VO) tool VOSA following the method described in Bayo et al. (2008).[7] The filled (red) circles represent the observed fluxes. The strong reddening is clearly seen. At the wavelength of the *V* filter (5500 Å), the SED flux is of the order of $10^{-18}$ erg s$^{-1}$ cm$^{-2}$ Å$^{-1}$ which corresponds to a magnitude of $V \sim 24$ mag, in agreement with the estimation in the previous section. For de-reddening the SED, we use the deduced $E(B - V)$ and the extinction law by Fitzpatrick (1999) improved by Indebetouw et al. (2005) in the infrared. The resulting de-reddened fluxes are shown as open (magenta) squares. Finally, we fitted the SED with the TLUSTY OSTAR2002+BSTAR2006 grid of stellar atmosphere models (Hubeny & Lanz 1995; Lanz & Hubeny 2003, 2007). The best fit (continuous, blue line) corresponds to a $T_{\text{Eff}} = 30\,000$ K and $E(B - V) = 4.94$. The IR excess above 3 μm is clearly seen (growing towards longer wavelengths). The bolometric luminosity for the IR counterpart can now be estimated from the ratio of observed to de-reddened fluxes.[8] This turns out to be

---

[7] Photometric fluxes provided through VO services (Bianchi & GALEX Team 2000; Ochsenbein, Bauer & Marcout 2000; Skrutskie et al. 2006; Wright et al. 2010; Ahn et al. 2012).

[8] Changing the log *g* had no noticeable effect in our fits given the uncertainties and the lack of data below 4000 Å.

**Table 3.** Extinctions and distances for the IGR J19294+1816 counterpart. Spectral type in the Morgan–Keenan system and intrinsic colours from Schmidt-Kaler ([1982](#)) and Ducati et al. ([2001](#)).

| MK | $(J-K)_0$ | $E^{\mathrm{tot}}(J-K)$ | $E^{\mathrm{is}}(J-K)^a$ | $M_K$ | $A_K^{\mathrm{is}}$ (mag) | $d$ (kpc) |
|---|---|---|---|---|---|---|
| B2Ve | −0.22 | 2.665 | 1.665 | −3.5 | 0.30 | 11.6[b] |
| B0Ve | −0.17 | 2.615 | 1.615 | −3.17 | 0.29 | 10.0[b] |

*Notes.* $^a E^{\mathrm{is}}(J\!-\!K) = E^{\mathrm{tot}}(J\!-\!K) - 1$.

$^b$ Assuming a saturated H$\alpha$ emission.
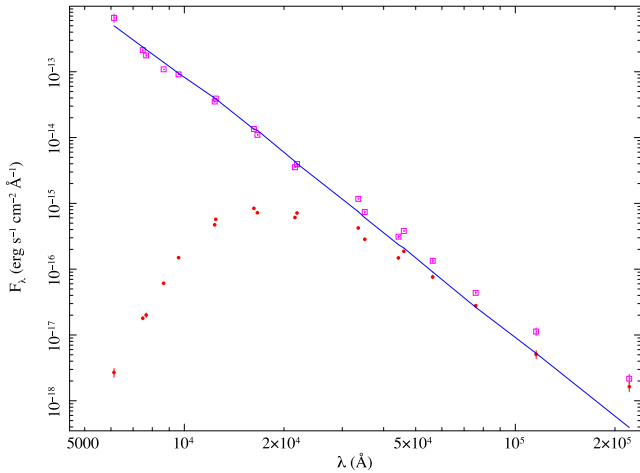


**Figure 6.** Spectral energy distribution of IGR J19294+1816. Filled circles represent the observed flux, open squares refer to the de-reddened flux with $E(B-V) = 4.94$, and continuous line is the best-fitting model.

$\approx 8 \times 10^{37}$ erg s$^{-1}$ = $(2.1 \pm 0.5) \times 10^4$ L$_\odot$. This is consistent with a B0–2 star of luminosity class V.

## 4 DISCUSSION AND CONCLUSIONS

IGR J19294+1816 is a transient system with a likely B1Ve donor. The unabsorbed X-ray flux (2–10 keV) reported by Rodriguez et al. ([2009a](#)) varies in the range of $(0.7–3.8) \times 10^{-11}$ erg s$^{-1}$ cm$^{-2}$ following the activity of the source with *INTEGRAL*, *RXTE* and *Swift*, while it reaches $5.4 \times 10^{-10}$ erg s$^{-1}$ cm$^{-2}$ in outburst (20–50 keV energy band) (Bozzo et al. [2011](#)). At the estimated distance of 11 kpc, the X-ray luminosity would be $(0.5–7.8) \times 10^{36}$ erg s$^{-1}$ in quiescence while the peak luminosity would be as high as $4.2 \times 10^{37}$ erg s$^{-1}$, assuming isotropic emission. The new NIR spectroscopy presented here as well as the *WISE* photometry analysis strongly favour a Be donor. Hence, our results, combined with the properties of the X-ray data, firmly classify IGR J19294+1816 as a Be-X-ray binary.

## REFERENCES

Ahn C. P. et al., 2012, ApJS, 203, 21
Bayo A., Rodrigo C., Barrado Y Navascués D., Solano E., Gutiérrez R., Morales-Calderón M., Allard F., 2008, A&A, 492, 277
Bianchi L., GALEX Team, 2000, Mem. Soc. Astron. Ital., 71, 1123
Blum R. D., Ramond T. M., Conti P. S., Figer D. F., Sellgren K., 1997, AJ, 113, 1855
Bozzo E., Ferrigno C., Falanga M., Walter R., 2011, A&A, 531, A65
Casali M. et al., 2007, A&A, 467, 777
Chambers K. C. et al., 2016, preprint (arXiv:1612.05560)
Drew J. E. et al., 2005, MNRAS, 362, 753
Ducati J. R., Bevilacqua C. M., Rembold S. B., Ribeiro D., 2001, ApJ, 558, 309
Esposito P., Israel G. L., Sidoli L., Mason E., Rodríguez Castillo G. A., Halpern J. P., Moretti A., Götz D., 2013, MNRAS, 433, 2028
Evans D. W. et al., 2017, A&A, 600, A51
Fitzpatrick E. L., 1999, PASP, 111, 63
Flewelling H. A. et al., 2016, preprint (arXiv:1612.05243)
Gaia Collaboration, 2016a, A&A, 595, A1
Gaia Collaboration, 2016b, A&A, 595, A2
Halpern J. P., Tyagi S., 2005, Astron. Telegram, 681
Hanson M. M., Conti P. S., Rieke M. J., 1996, ApJS, 107, 281
Hanson M. M., Rieke G. H., Luhman K. L., 1998, AJ, 116, 1915
Hanson M. M., Kudritzki R.-P., Kenworthy M. A., Puls J., Tokunaga A. T., 2005, ApJS, 161, 154
Hubeny I., Lanz T., 1995, ApJ, 439, 875
Indebetouw R. et al., 2005, ApJ, 619, 931
Kaur R., Paul B., Kumar B., Sagar R., 2008, MNRAS, 386, 2253
Koenig X. P., Leisawitz D. T., 2014, ApJ, 791, 131
Lanz T., Hubeny I., 2003, ApJS, 146, 417
Lanz T., Hubeny I., 2007, ApJS, 169, 83
Lawrence A. et al., 2007, MNRAS, 379, 1599

Magnier E. A. et al., 2016a, preprint (arXiv:1612.05240)
Magnier E. A. et al., 2016b, preprint (arXiv:1612.05244)
Magnier E. A. et al., 2016c, preprint (arXiv:1612.05242)
Mainzer A. et al., 2011, ApJ, 731, 53
Mainzer A. et al., 2014, ApJ, 792, 30
Martínez-Núñez S. et al., 2017, Space Sci. Rev., 212, 59
Masetti N. et al., 2006, A&A, 455, 11
Masetti N., Jimenez-Bailon E., Chavushyan V., Parisi P., Bazzano A., Landi R., Bird A. J., 2012, Astron. Telegram, 4248
Meyer M. R., Edwards S., Hinkle K. H., Strom S. E., 1998, ApJ, 508, 397
Ochsenbein F., Bauer P., Marcout J., 2000, A&AS, 143, 23
Reig P., 2011, Ap&SS, 332, 1
Riquelme M. S., Torrejón J. M., Negueruela I., 2012, A&A, 539, A114
Rodes-Roca J. J., Torrejón J. M., Martínez-Núñez S., Bernabéu G., Magazzú A., 2013, A&A, 555, A115
Rodriguez J., Tomsick J. A., Bodaghee A., Zurita Heras J.-A., Chaty S., Paizis A., Corbel S., 2009a, A&A, 508, 889
Rodriguez J., Tuerler M., Chaty S., Tomsick J. A., 2009b, Astron. Telegram, 1998
Schmidt-Kaler T., 1982, in Aller L. H. et al., eds, Landolt-Bornstein: Group 6: Astronomy and Astrophysics, Vol. 2 Schaifers/Voigt. Springer-Verlag, New York

Sidoli L., Israel G. L., Esposito P., Rodríguez Castillo G. A., Postnov K., 2017, MNRAS, 469, 3056
Skrutskie M. F. et al., 2006, AJ, 131, 1163
Slettebak A., Collins G. W., II, Truax R., 1992, ApJS, 81, 335
Steele I. A., Clark J. S., 2001, A&A, 371, 643
Strohmayer T., Rodriquez J., Markwardt C., Tomsick J., Bodaghee A., Chaty S., Corbel S., Paizis A., 2009, Astron. Telegram, 2002
Turler M., Rodriguez J., Ferrigno C., 2009, Astron. Telegram, 1997
Underhill A., Doazan V., 1982, J. Br. Astron. Assoc., 92, 290
van Leeuwen F. et al., 2017, A&A, 599, A32
Waters C. Z. et al., 2016, preprint (arXiv:1612.05245)
Watson M. G. et al., 2009, A&A, 493, 339
Wenger M. et al., 2000, A&AS, 143, 9
Winkler C. et al., 2003, A&A, 411, L1
Wright E. L. et al., 2010, AJ, 140, 1868

This paper has been typeset from a TEX/LATEX file prepared by the author.